

# Femtosecond laser inscription of nonlinear photonic circuits in Gallium Lanthanum Sulphide glass

María Ramos Vázquez<sup>1,2</sup>, Belén Sotillo<sup>3,4</sup> Stefano Rampini<sup>3</sup>, Vibhav Bharadwaj<sup>3,5</sup>, Behrad Gholipour<sup>6</sup>, Paloma Fernández<sup>4</sup>, Roberta Ramponi<sup>3</sup>, Cesare Soci<sup>2</sup> and Shane M. Eaton<sup>3</sup>

<sup>1</sup> ICRM, Interdisciplinary Graduate School, Nanyang Technological University, Singapore

<sup>2</sup> Centre for Disruptive Photonic Technologies, TPI, Nanyang Technological University, Singapore

<sup>3</sup> Institute for Photonics and Nanotechnologies (IFN) - CNR, Milano, Italy

<sup>4</sup> Dept. Física de Materiales, Fac. Físicas, U. Complutense, Ciudad Universitaria, Madrid, Spain

<sup>5</sup> Center for Nano Science and Technology, Istituto Italiano di Tecnologia, Milano, Italy

<sup>6</sup> Optoelectronics Research Centre, University of Southampton, UK

E-mail: shane.eaton@gmail.com

## Abstract

We report on femtosecond laser writing of single mode optical waveguides in chalcogenide Gallium Lanthanum Sulfide (GLS) glass, a substrate with great promise for nonlinear photonics. A multiscan fabrication process was adopted to create waveguides with symmetric single mode guidance and low insertion losses at 800 nm wavelength, compatible with Ti:Sapphire ultrafast laser technology. The laser induced modifications were further characterized via  $\mu$ Raman and EDX spectroscopy. Nonlinear refractive index measurements of the waveguides were performed by finding the optical switching parameters of a directional coupler in order to demonstrate that the nonlinear properties of GLS are preserved.

Keywords: Ultrafast laser writing, chalcogenides, optical switching, Kerr effect

---

## 1. Introduction

Nonlinear optical processes gained increasing attention in the past decade as the basis for innovative technologies in optics and photonics and in particular for all-optical signal processing [1]. The highly nonlinear properties of chalcogenide glasses, i.e. glasses made of one or more chalcogen elements (O, S, Se, Te, Po) and network formers (such as As, Ge, Sb, Ga, Si or P), have attracted great interest as a nonlinear photonics platform: they have high linear and nonlinear refractive indices, a wide transparency window up to the infrared (IR) region of the spectrum, a low maximum phonon energy and an ultrafast nonlinear response time in the

femtoseconds range [2]. Among the chalcogenides, commercially available Gallium Lanthanum Sulfide (GLS) has the highest nonlinear figure of merit [3], being thermally stable up to 550°C, and does not present toxicity related issues as other commonly used chalcogenide glasses such as As<sub>2</sub>Se<sub>3</sub>.

Several approaches are available for creating optical circuits in chalcogenide glasses, such as thin films, microspheres or optical fibers [4]. Of particular interest is the fabrication of waveguides and other optical components via femtosecond laser inscription [5]. This technology relies on the nonlinear absorption of ultrashort laser pulses focused in the bulk of the material. The nonlinearity of the process leads to a

---

localized modification which, in most glasses generates a positive refractive index change. The translation of the sample in three dimensions with respect to the incident laser beam generates complex buried geometries which would not be achievable with other techniques.

Previous examples of waveguides in chalcogenide glasses have been targeted for mid IR wavelengths, reporting low losses (0.65 dB/cm) by using spatial beam shaping and temporal pulse optimization [6]. Also, prior related work showed single mode guidance at 633 nm and 1550 nm in GeGaS glass [7, 8]. In addition, femtosecond inscribed mid-IR directional couplers for optical astronomical applications were reported at 3.39  $\mu\text{m}$  wavelengths [9].

Here we report the femtosecond laser writing of buried waveguides in GLS designed for the convenient 800 nm band, where Ti:Sapphire technology offers ultrashort laser pulses. The cross sectional profile of the inscribed waveguides was controlled using the multiscan shaping approach, thus generating a more symmetric profile [8]. To gain further insight into the laser interaction physics, the modifications were analyzed using micro-Raman ( $\mu\text{Raman}$ ) and Energy dispersion X-ray measurements (EDX) spectroscopy. Furthermore, optical directional couplers were laser written and showed to work as nonlinear optical switches, with the nonlinear refractive index of the waveguides deduced from the optical switching parameters. The results presented here represent the first demonstration photonic circuits in chalcogenides at 800 nm wavelength.

## 2. Materials and methods

### 2.1 Femtosecond laser inscription of GLS waveguides

The femtosecond second laser used for waveguide writing in GLS was a regeneratively amplified Yb:KGW system (Pharos, Light Conversion) with 230 fs pulse duration, 1030 nm wavelength, focused with a 0.42 NA microscope objective (M Plan Apo SL50X Ultra-Long Working Distance Plan-Apochromat, Mitutoyo). The repetition rate of the laser was variable from 1 MHz to single pulse but for the laser writing experiments was held fixed at 500 kHz. Computer-controlled, 3-axis motion stages (ABL-1000, Aerotech) interfaced by CAD-based software (ScaBase, Altechna) with an integrated acousto-optic modulator (AOM) were used to translate the sample relative to the laser to form the desired

photonic structures. The waveguides were inscribed in transverse geometry, with the sample translated perpendicular to the propagation direction of the laser. The polarization of the incident laser was perpendicular to the scan direction.

Waveguides were inscribed at a depth of 150  $\mu\text{m}$ , with incident laser power  $P$  ranging from 10 mW to 250 mW (laser pulse energies from 20 nJ to 500 nJ). Each waveguide consisted of 18 consecutive laser scans separated by 0.3  $\mu\text{m}$ . Four translations speeds  $v = 5, 10, 20, \text{ and } 50 \text{ mm/s}$  were used to inscribe each batch of waveguides. The sample facets were polished after the inscription for an optimum optical quality. Sets of directional couplers were fabricated with an input-to-input port distance  $p = 100 \mu\text{m}$ , from core to core,  $R = 45 \text{ mm}$  bend radius and a center to center separation distance in the interaction region of  $s = 7 \mu\text{m}$ . The interaction length  $L$  were varied between 0 and 2 mm in steps of 0.25 mm.

### 2.2 Waveguide and directional coupler characterization

Waveguide transmission measurements were performed by using fiber – butt coupled strategy. High resolution 3-axis manual positioners (Nanomax MAX313D, Thorlabs) were used for fiber in and fiber out alignments. The four-axis central waveguide manipulator (MicroBlock MBT401D, Thorlabs) enabled transverse displacement between sets of waveguides in the sample. A light source at 808 nm (S1FC808, Thorlabs) was coupled to the waveguides using single-mode fiber (780HP, Thorlabs). At the output, light was coupled to an optical power meter (818-SL, Newport) to measure the power transmitted through the waveguide. To measure the near-field waveguide mode profile, a 60 $\times$  asphere (5721-H-B, Newport) was used to image the light onto a beam profiler (SP620U, Spiricon).

### 2.3 Nonlinear characterization as all-optical switches

An all-optical switch is a device that allows the control of an optical signal through the use of another optical signal. In this case, the nonlinear directional couplers act as an ultrafast all-optical switching device due to the power control of a unique input signal. The foundation of all-optical switching relies on the refractive index change of the material, induced by the nonlinear Kerr effect. In this concern, all-optical switching is manifested as an intensity dependent refractive index induced in the nonlinear material [10]:

$$n = n_0 + n_2 I,$$

where  $n_0$  is the linear refractive index,  $n_2$  is the nonlinear refractive index and  $I$  is the intensity of the control light.

When an intense electromagnetic field propagates through the glass waveguide, a nonlinear polarization manifests itself in the medium and subsequently modifies the propagation properties of the light. In the case of GLS glass, this nonlinear effect occurs because of the high third order hyperpolarizability of the sulphide ion [4].

Therefore, the light propagation through a directional coupler will periodically alternate from one waveguide to the other one while the input irradiance changes. At low input irradiances, the propagation of light will remain in the linear regime. At high input irradiances, the nonlinear effect induced in the medium will lead to self-focusing or self-trapping causing most of the light to remain in the through output port waveguide [11].

For finding the optical switching in different directional couplers, a single beam experiment was performed. A home built amplified Ti:Sapphire laser system operating at 2 kHz repetition rate, 180 fs pulsewidth and 800 nm center wavelength was used to couple the light into one of the input ports of the directional couplers by focusing the light with a 0.16-NA antireflection coated objective lens. A 0.25-NA microscope objective was used to collect the output guided modes from the end facet of the glass sample and subsequently light was sent into a Si CCD camera for power detection (SP620U, Spiricon). The light power at the input was measured by using a silicon photodetector placed right before the focusing objective lens.

#### 2.4 Raman studies

In order to gain better understanding of the waveguide formation in bulk GLS,  $\mu$ Raman measurements have been performed. The  $\mu$ Raman spectra were recorded in a Horiba JovinYvon LabRAM HR800 confocal microscope, equipped with an air-cooled CCD. The excitation wavelength was 633 nm from a He-Ne laser source. A 100 $\times$  (0.9NA) objective

was used to focus the laser on the sample as well as to collect the Raman spectra (backscattering configuration), with a spatial resolution below 1  $\mu$ m.

#### 2.5 EDX compositional analysis

EDX has been performed to study the compositional element analysis of the laser formed waveguides. EDX measurements have been done in a Bruker Quantax 70 EDS system attached to a scanning electron microscope Hitachi TM3000, operated at 15 kV. The energy resolution for this system is around 154 eV (for Cu K $\alpha$ ). Backscattered electron (BSE) images were taken also in the Hitachi TM300 SEM.

### 3. Results and discussion

#### 3.1 Waveguide characterization

Figure 1 shows the cross-sectional (a) and overhead (b) microscopic view and near field mode profile (c) for the lowest loss waveguide, formed with a pulse energy of 70 nJ and a scan speed of 5 mm/s. For energies above 75 nJ, the waveguides were multimode. The insertion loss was 1.9 dB and the mode field diameter of 8.5  $\mu$ m.

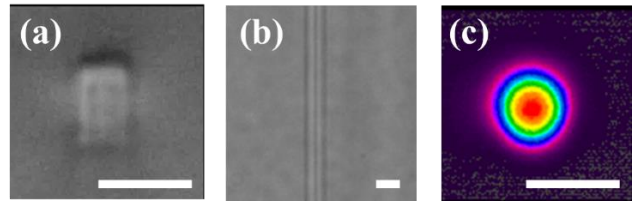


**Fig. 1.** Transverse (a) and overhead (b) microscope view of the waveguide written with a laser energy of 70 nJ and a scan speed of 5 mm/s. (c) The guided mode for the specific waveguide at 808 nm wavelength guidance. The scale bar corresponds to 10  $\mu$ m.

#### 3.2 Directional couplers characterization

A directional coupler consists of two S-bends which bring two waveguides in close proximity to enable evanescent light coupling (Fig. 3). In order to choose the optimum radius of curvature for the S-bends, a study of bend loss with varying radius of curvature was performed. The bend loss was calculated by subtracting the insertion loss of the straight waveguide from the insertion loss of the two S-bends making up one arm of the directional couplers. Figure 2 shows the bend loss versus radius of curvature. As expected, larger bend radii offer lower losses, but result in longer axial length of the S-bends, increasing the overall size of the chip (defined as axial footprint of a directional coupler with

zero interaction length). A compromise between the losses and the size of the chip was obtained with a radius of curvature of 45 mm.

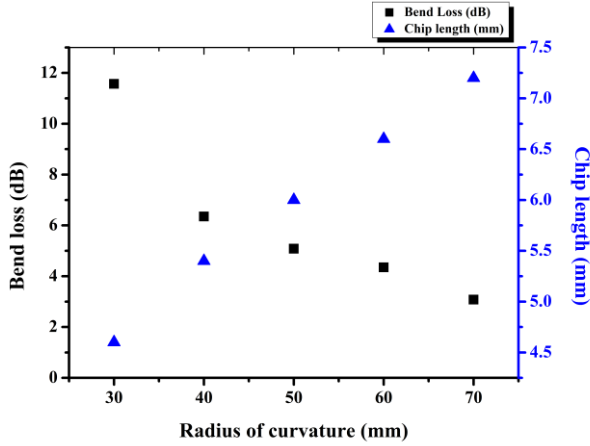


**Fig. 2.** Measured bend loss of two S bends and chip length (two S bends with zero interaction length) versus radius of curvature.

Symmetric directional couplers were laser written in the bulk of GLS sample with varying interaction length  $L$  for  $R = 45$  mm and separation between the waveguides in the interaction region  $s = 7$   $\mu\text{m}$  as shown in Fig. 3(a). The optimum parameters (pulse energy 70 nJ and scan speed 5 mm/s) for straight waveguide fabrication were used to fabricate the couplers. The separation between the ports  $p$  was fixed at 100  $\mu\text{m}$ , a convenient separation for fiber characterization.

The laser written directional couplers were characterized by launching in fiber coupled 808 nm wavelength into one of the arm and measuring the power in the cross and through output ports. A plot of coupling ratio versus the interaction length was obtained, as shown in Fig. 3(b). This plot was well fitted in a sin squared function according to the equation  $\text{CR} = \sin^2\left(\frac{\pi}{l_B(\lambda)}L\right)$ , where CR is the power coupling ratio,  $l_B$  the coupler beat length,  $\lambda$  the wavelength and  $L$  the interaction length. The peak coupling ratio obtainable was 54%, less than the ideal 100%, which is due to differing propagation constants of the two waveguides forming the directional coupler [12]. As the waveguides were fabricated in the non-heat accumulation regime with multiple passes, the waveguides are more sensitive to any fluctuations during fabrication compared to waveguides written with the cumulative heating process [12]. Further optimization of the laser-written waveguides could lead to an increase in this peak coupling ratio.

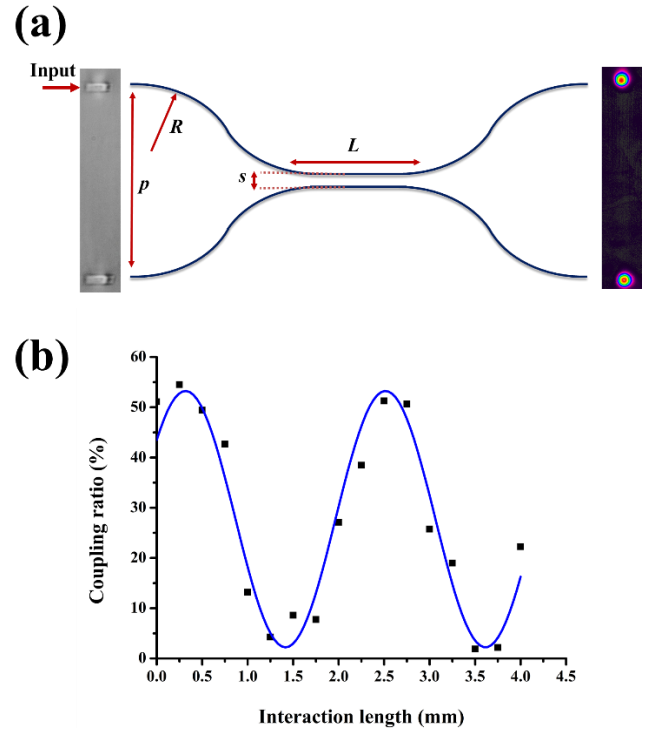


**Fig. 3.** (a) Sketch of a symmetric directional coupler showing the various parameters defining it radius of curvature  $R$ , interaction length  $L$ , center to center separation between the waveguides in the interaction region  $s$ , separation between the two ports  $p$ . On the left, a side view optical microscope image of the two input ports is shown and, on the right, the output modes measured for a directional coupler with 50% coupling ratio is shown. (b) Plot of coupling ratio with respect to the interaction length with the sin squared fitting represented in blue.

### 3.3 Deduction of $n_2$ from switching parameters

The directional coupler selected for the measurement of the nonlinear refractive index had an interaction length  $L = 250$   $\mu\text{m}$ . The relative transmission of the through and cross output waveguide ports as a function of the input irradiance is shown in Fig. 4. The switching input irradiance needed to achieve the same power in the through (bar) and cross ports was  $7.1 \times 10^{15}$   $\text{W}/\text{m}^2$ . For lower input irradiances, most of the light was evanescently coupled into the cross waveguide, with a relative transmission of the cross output port at 54%. For values above the switching irradiance, most of the light propagation takes place along the through waveguide, with a relative transmission of the cross output port decreasing to 48%.

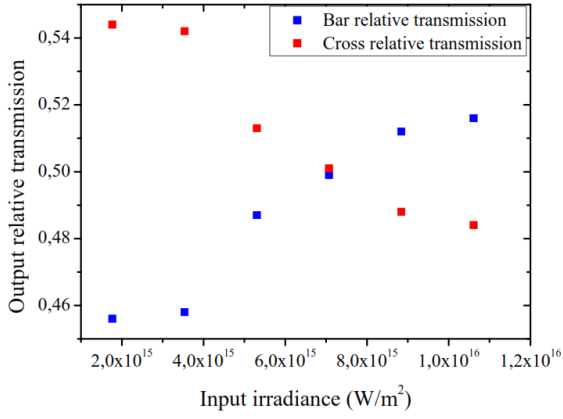


**Fig. 4.** Bar and cross output relative transmissions as a function of input irradiance. The point at which the output relative transmissions become equal occurs at  $7.1 \times 10^{15} \text{ W/cm}^2$ .

The nonlinear phase change induced within the directional coupler, due to nonlinear refraction, is given by [13]:

$$\Delta\phi = \frac{2\pi L n_2 I}{\lambda},$$

where  $L$  is the interaction length of the directional coupler,  $n_2$  is the nonlinear refractive index of the waveguide,  $I$  is the input irradiance and  $\lambda$  is the operating wavelength.

Taking into account that the phase change required to switch a nonlinear directional coupler is approximately  $4\pi$  [14] and considering the Fresnel losses at the input facet of the waveguide, an evaluation of the nonlinear refractive index of the laser written waveguides can be performed. Specifically, for the directional coupler chosen, the nonlinear refractive index of the waveguide is equal to  $9.0 \times 10^{-19} \text{ m}^2/\text{W}$ . The nonlinear refractive index value of the laser inscribed waveguides is on the same order of magnitude as the nonlinear refractive index of pristine GLS reported previously [4].

### 3.2 Structural and compositional characterization

Initial characterization of the pristine glass has been performed to understand the changes that the femtosecond laser writing is producing in the material. In Fig. 5(a) the absorption spectrum of a sample is

shown, where the absorption edge is around 515 nm, similar to previously reported values [15]. An EDX spectrum is presented in Fig. 5(b), confirming the presence of S, Ga, and La in a proportion 4:2:1. EDX measured at different points and in different samples indicate a uniform distribution of the three elements. No oxygen signal was detected.

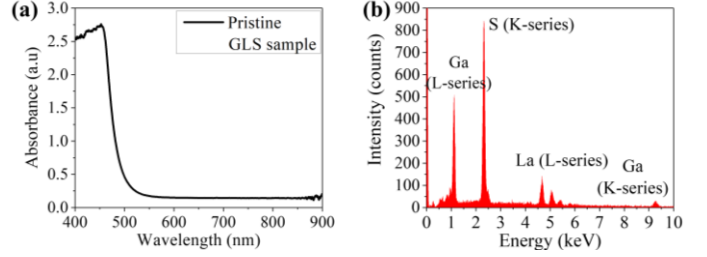


**Fig. 5.** (a) Absorbance and (b) EDX spectra of pristine GLS.

Before explaining the Raman spectra recorded in GLS glass, a brief description of the glass network is needed to understand the spectra. Ga atoms are bonded to sulfur forming tetrahedral networks of  $\text{GaS}_4$ , which are the glass units.  $\text{S}^{2-}$  anions provided by the modifying lanthanum sulfide maintain the tetrahedral environment of  $\text{GaS}_4$ , as gallium sulfide alone cannot form a glass. The negatively charged  $\text{GaS}_4$  tetrahedra are reception sites for  $\text{La}^{3+}$  cations [16].

The Raman spectra of the GLS glass is then generally dominated by the modes associated to the  $\text{GaS}_4$  tetrahedra vibrations [17, 18]. As shown Fig. 6, the main band is located between 250 and  $450 \text{ cm}^{-1}$  and centered at  $325 \text{ cm}^{-1}$ . Other bands are also visible in the region  $100 - 250 \text{ cm}^{-1}$ . The dominant band at  $325 \text{ cm}^{-1}$  is ascribed to symmetrical stretching vibrations of the  $\text{GaS}_4$  units, whereas the band at  $140 \text{ cm}^{-1}$  is associated to the asymmetrical bending. Band around  $100 \text{ cm}^{-1}$  and  $380 \text{ cm}^{-1}$ , which are less defined in the spectrum, come from the symmetrical bending and the asymmetrical bending, respectively. The band related to the La-S vibration is found at  $215 \text{ cm}^{-1}$  [19]. There is no evidence of crystallization in the Raman spectra taken in the pristine material as well as in the spectra of the waveguides.

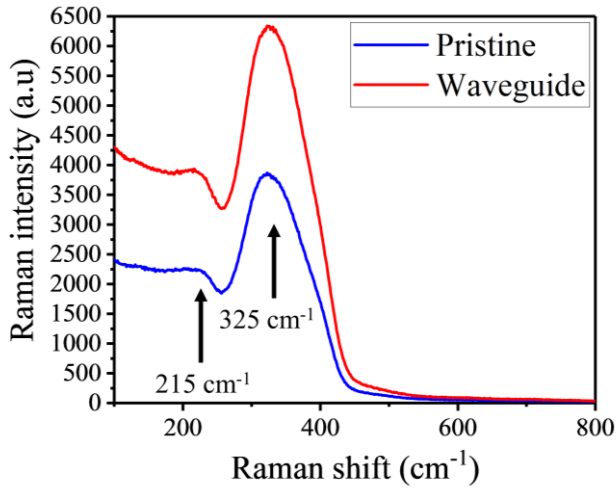


Fig. 6.  $\mu$ Raman spectra recorded on pristine GLS (blue curve) and on a waveguide (red curve) written with a laser energy of 70 nJ and a scan speed of 5 mm/s. The excitation wavelength is 633 nm.

In the  $\mu$ Raman spectra recorded inside the waveguides (Fig. 7), there are two main effects observed. The first effect is the increase of the total Raman signal (Fig. 6 and 7(a)). The second observation is the increase of the relative intensity of the band associated with La-S bonds at 215  $\text{cm}^{-1}$  (Fig. 7(b)-(c)). Also, slightly changes of relative intensity of the different vibration modes of the  $\text{GaS}_4$  tetrahedra are observed. These variations of the  $\mu$ Raman spectra are uniform inside the region of the waveguide, as shown in the maps of Fig. 7(a)-(c).

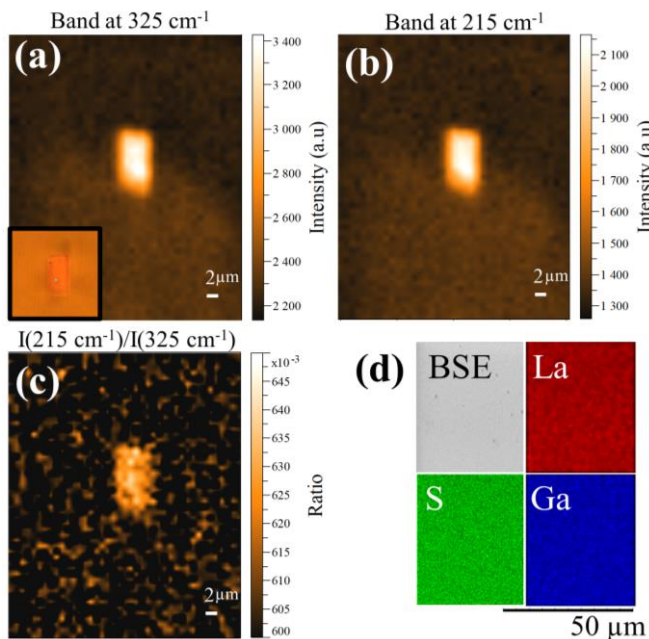


Fig. 7. (a)-(c)  $\mu$ Raman maps of different bands in a waveguide written with a laser energy of 70 nJ and a scan speed of 5 mm/s. (a) Intensity of the band at 325  $\text{cm}^{-1}$  (symmetrical stretching vibrations of the  $\text{GaS}_4$  units). The inset shows the transverse optical microscope image of the waveguide. (b) Intensity of the band at 215  $\text{cm}^{-1}$  (La-S bond vibrations). (c) Intensity ratio of the 215  $\text{cm}^{-1}$  and 325  $\text{cm}^{-1}$  band. All the scale bars are 2  $\mu\text{m}$ . (d) BSE image and EDX maps of the different elements (La in red, S in green, Ga in blue).

The changes in the relative intensity of the  $\text{GaS}_4$  related modes is related to slightly deformations of the bondings of the tetrahedral (i.e. bonding angles). Also the increase of the total Raman intensity is related to a deformation of the bondings in the GLS network, which produces an increase of polarizability and/or density of the material in the waveguide. This produces the observed increase in the refractive index. The increase of the relative intensity of the La-S vibration band is related to the break of Ga-S bonds and the formation of new La-S bonds.

In other waveguides fabricated with femtosecond laser writing in glasses containing lanthanum, there has been observed an ion migration that produces the increase in the refractive index [19,20]. For the GLS system of this work, and for all the waveguides studied, no Z-contrast is observed in the BSE images, which suggests that the laser did not produce a strong elemental compositional change in the irradiated glass network. It is possible that higher fluences which could drive heat accumulation would lead to a migration of ions in GLS. From the EDX measurements, presented in Fig. 8(d) (La in red, S in green and Ga in blue) no significant migration of the elements is observed inside the waveguide. These observations are in agreement with previously reported EDX studies performed in GLS waveguides, where no compositional changes were detected [21]. Then, from EDX and Raman measurements, the laser is inducing changes of the Ga-S and La-S bondings in the focal volume, producing a rearrangement of the glass network that lead to an increase in the refractive index.

As we have described before, if the pulse energy used to fabricate the waveguides is too high, dark filaments appear around the waveguide. The Raman signal in these darker region decreases (see Fig. 8(a)-(b)), an effect that is typically associated with extended defects formation and broken bonds [18]. So if the pulse energy

is too high, the glass is not able to rearrange the bonds and the glass network suffers an expansion (evidenced also in the BSE images with a swollen region at the surface, not shown) and a decrease of the refractive index. This is the opposite effect to the one observed for low pulse energies. Further increment of the laser power produces a high damage in the glass, expanding the glass network and creating voids that sometimes emerge to the surface, as shown in the BSE image of Fig. 8(c). EDX map of Fig. 8(d) show that the material (mainly Ga and S) is ejected outside the laser-written tracks. The creation of voids for higher pulse energies fabrication has been also been observed in other glasses like fused silica [22].

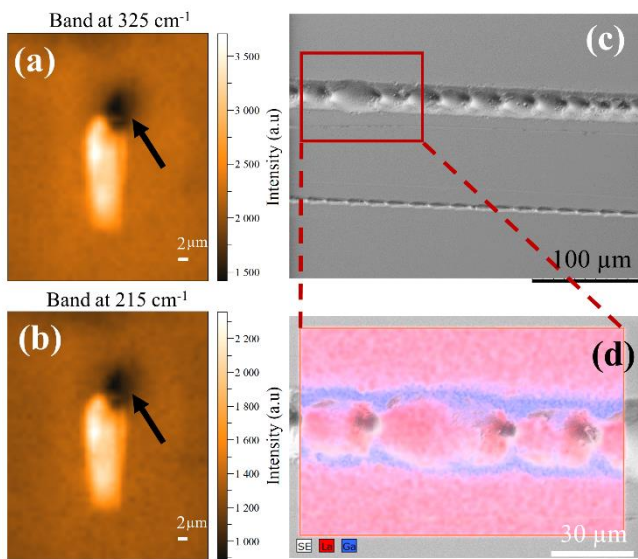


Figure 8. (a)-(b)  $\mu$ Raman maps of different bands in a waveguide written with a laser energy of 200 nJ and a scan speed of 10 mm/s. (a) Intensity of the band at 325  $\text{cm}^{-1}$ . (b) Intensity of the band at 215  $\text{cm}^{-1}$ . (c) BSE image of a laser track fabricated with 400 nJ pulse energy. The compositional map of a selected area is shown in (d) (La in red, Ga in blue).

#### 4. Summary

In summary, we fabricated waveguides in GLS using focused femtosecond laser pulses, demonstrating single mode guidance and an insertion loss of 1.9 dB. Ultrafast all-optical switching was performed at the femtosecond regime by the laser written directional couplers and an evaluation of their nonlinear refractive index was obtained from the switching parameters. The nonlinear refractive index value of the laser inscribed waveguides is on the same order of magnitude of the

pristine material ( $n_2 = 2.16 \times 10^{-19} \text{ m}^2/\text{W}$ ) reported in previous literature, [4]. EDX and Raman measurements performed in the waveguides show that the laser irradiation is producing a gentle modification of the GLS network, altering the Ga-S and La-S bonds to create a region with higher polarizability and/or density, inducing the increase in the refractive index observed.

#### Acknowledgements

We are grateful to Luigino Criante for access to the FemtoFab facility at CNST-IIT Milano for the laser fabrication experiments. We appreciate the funding sources of Singapore Ministry of Education (MOE2011-T3-1-005), DIAMANTE MIUR-SIR Grant and FemtoDiamante Cariplo ERC Reinforcement Grant. B. Sotillo acknowledges financial support from Comunidad de Madrid (Ayudas atracción de talento) and MINECO/FEDER-MAT2015-65274-R Project.

#### References

1. A. E. Willner, S. Khaleghi, M. R. Chitgarha, and O. F. Yilmaz, "All-optical signal processing," *Journal of Lightwave Technology* **32**, 660-680 (2014).
2. A. Zakery and S. Elliott, "Optical properties and applications of chalcogenide glasses: a review," *Journal of Non-Crystalline Solids* **330**, 1-12 (2003).
3. J. Requejo-Isidro, A. Mairaj, V. Pruneri, D. Hewak, M. Netti, and J. Baumberg, "Self refractive non-linearities in chalcogenide based glasses," *Journal of non-crystalline solids* **317**, 241-246 (2003).
4. Hewak, D.W. & Brady, D & Curry, Richard & Elliott, Gregor & Huang, Kevin Chung-Che & Hughes, Mark & Knight, Kiara & Mairaj, A & Petrovich, M.N. & Simpson, Robert & Sproat, C. (2010). Chalcogenide glasses for photonics device applications.
5. B. McMillen, B. Zhang, K. P. Chen, A. Benayas, and D. Jaque, "Ultrafast laser fabrication of low-loss waveguides in chalcogenide glass with 0.65 dB/cm loss," *Optics letters* **37**, 1418-1420 (2012).
6. M. Hughes, W. Yang, and D. Hewak, "Fabrication and characterization of femtosecond laser written waveguides in chalcogenide glass," *Applied Physics Letters* **90**, 131113 (2007).
7. A. Ayiriveetil, T. Sabapathy, G. S. Varma, U. Ramamurty, and S. Asokan, "Structural and mechanical characterization on ultrafast laser written chalcogenide glass waveguides," *Optical Materials Express* **6**, 2530-2536 (2016).

- 
8. Arriola, A., Mukherjee, S., Choudhury, D., Labadie, L. and Thomson, R.R., 2014. Ultrafast laser inscription of mid-IR directional couplers for stellar interferometry. *Optics Letters*, 39(16), pp.4820-4822.
  9. T. Gretzinger, S. Gross, M. Ams, A. Arriola, and M. J. Withford, "Ultrafast laser inscription in chalcogenide glass: thermal versus athermal fabrication," *Optical Materials Express* 5, 2862-2877 (2015).
  10. Tanaka, K., 2017. Optical nonlinearity in photonic glasses. In *Springer Handbook of Electronic and Photonic Materials* (p. 1083). Springer, Cham.
  11. Boyd, R.W., 2003. *Nonlinear optics*. Academic press.
  12. S. M. Eaton, W. Chen, L. Zhang, H. Zhang, R. Iyer, J. S.Aitchison, and P. R. Herman, *IEEE Photon. Technol. Lett.* 18, 2174 (2006).
  13. Demetriou, G., Hewak, D.W., Ravagli, A., Craig, C. and Kar, A., 2017. Nonlinear refractive index of ultrafast laser inscribed waveguides in gallium lanthanum sulphide. *Applied optics*, 56(19), pp.5407-5411.
  14. Stegeman, G.I., Wright, E.M., Finlayson, N., Zaroni, R. and Seaton, C.T., 1988. Third order nonlinear integrated optics. *Journal of lightwave technology*, 6(6), pp.953-970.
  15. Brady, D. J., Schweizer, T., Wang, J., & Hewak, D. W. (1998). Minimum loss predictions and measurements in gallium lanthanum sulphide based glasses and fibre. *Journal of non-crystalline solids*, 242(2-3), 92-98.
  16. A. Zakery, S.R. Elliott, "Optical Nonlinearities in Chalcogenide Glasses and their Applications"; *Springer Series in Optical Science* (2007)
  17. Schweizer, T., Goutaland, F., Martins, E., Hewak, D. W., & Brocklesby, W. S. (2001). Site-selective spectroscopy in dysprosium-doped chalcogenide glasses for 1.3- $\mu\text{m}$  optical-fiber amplifiers. *JOSA B*, 18(10), 1436-1442.
  18. Heo, J., Yoon, J. M., & Ryou, S. Y. (1998). Raman spectroscopic analysis on the solubility mechanism of  $\text{La}^{3+}$  in  $\text{GeS}_2\text{-Ga}_2\text{S}_3$  glasses. *Journal of non-crystalline solids*, 238(1-2), 115-123.
  19. Fernandez, T. T., Haro-González, P., Sotillo, B., Hernandez, M., Jaque, D., Fernandez, P., ... & Solis, J. (2013). Ion migration assisted inscription of high refractive index contrast waveguides by femtosecond laser pulses in phosphate glass. *Optics letters*, 38(24), 5248-5251.
  20. del Hoyo, J., Vazquez, R. M., Sotillo, B., Fernandez, T. T., Siegel, J., Fernández, P., ... & Solis, J. (2014). Control of waveguide properties by tuning femtosecond laser induced compositional changes. *Applied Physics Letters*, 105(13), 131101.
  21. Hughes, M. A., Yang, W., & Hewak, D. W. (2009). Spectral broadening in femtosecond laser written waveguides in chalcogenide glass. *JOSA B*, 26(7), 1370-1378.
  22. Toratani, E., Kamata, M., & Obara, M. (2005). Self-fabrication of void array in fused silica by femtosecond laser processing. *Applied Physics Letters*, 87(17), 171103.